

# A quantum algorithm for finding collision-inducing disturbance vectors in SHA-1

**Jiheng Duan**

Department of Physics and Chemistry, Faculty of Science and Technology,  
University of Macau, Macau SAR, China

**Minghui Li**

Institute of Applied Physics and Materials Engineering, University of Macau,  
Macau SAR, China

**Hou Ian**

Institute of Applied Physics and Materials Engineering, University of Macau,  
Macau SAR, China

E-mail: houian@um.edu.mo

**Abstract.** Modern cryptographic protocols rely on sophisticated hash functions to generate quasi-unique numbers that serve as signatures for user authentication and other security verifications. The security could be compromised by finding texts hash-mappable to identical numbers, forming so-called collision attack. Seeding a disturbance vector in the hash mapping to obtain a successful collision is that a major focus of cryptography study in the past two decades to improve hash protocols. We propose an algorithm that takes advantage of entangled quantum states for concurrent seeding of candidate disturbance vectors, out of which the one entailing collision is selected through a combination of quantum search, phase gating, diffusion gating, and information feedbacks from classical computing machinery. The complexity reduction is shown to be on the order of  $\mathcal{O}(2^{n/2+1})$  where  $n$  is the number of qubits encoding addresses. We demonstrate the practicality of the proposed by an implementation scheme based on degenerate optical parametric oscillators.

## 1. Introduction

Cryptographic hash functions appeared at the end of the twentieth century and became one of the most significant concepts in key derivation, password hashing, and digital signatures which were popularized since 1990s [1]. The most ubiquitous cryptographic hash functions belong to the secure hash algorithm (SHA) family [2], which includes the variants SHA-0 up to SHA-3. The SHA function converts input messages into quasi-unique and orderless strings of a fixed length. Since this length is much shorter than the lengths of original messages, collisions are doomed to occur due to the pigeon-hole principle, where two or more messages are converted to the same hash value. The careful design of the SHA family, however, mandates that similar messages lead to vastly distinct hash values, let alone messages of different lengths. It was believed that hash collisions would never occur such that authentication systems would be protected from fake signatures from malware. The course took a sudden change in 2005 when the first practical collision attack of SHA-1 was proposed by employing a differential path method [3, 4]. Since then, more collision attacks have been found with relatively low algorithmic complexities. Constructing differential paths essentially reduces the time complexity of finding collision-inducing messages from brute-force method and the introduction of disturbance vectors (DV) further simplifies this construction [5, 6, 7, 8]. Hence, finding the DVs becomes the key to finding the collision attacks on SHA-1 [9].

Despite the reduction in complexity, finding DV still remains a computationally daunting task in a practice sense and often seeking a collision relies on heuristic approaches. Quantum algorithms, nevertheless, poses unparalleled advantage over classical algorithms in tackling specific computational problems. The use of quantum computers would render some classically improbable tasks tangible, granting the programmer quantum supremacy [10]. Two particularly well-known problems falling in this category are the factorization of large integers, solved by Shor’s algorithm [11], and the searching in unsorted list, solved by Grover’s algorithm [12]. The latter has been applied in numerous works to enhance computation efficacy [13, 14, 15]. Therefore, it is only natural to take advantage of quantum parallelism to improve the efficacy of seeking SHA-1 collisions but, to our knowledge, scarcely have such quantum approaches been attempted. A quantum collision search that elevates from classical semi-free-start collisions [16, 17] on reduced SHA-256 and SHA-512 was proposed last year [18].

Here, we propose a quantum algorithm for seeding DVs against SHA-1, which combines diffusion and inversion gating from Grover’s algorithm, quantum phase gating, diffusion gating, and information feedback from classical computing machinery, to greatly reduce the overall computation complexity. The algorithm runs on a quantum machine of two  $n = 16\lambda$  qubit-long registers  $R_C$  and  $R_W$ , where  $\lambda$  is the bit weight of the candidate DVs. While the control register  $R_C$  stores the addresses of the DVs, the work register  $R_W$  carries the hash computation related information. The principles of the algorithm apply to other SHA and MD5 hashing protocols as well, only that the qubit length would vary. The concurrency of searching permitted by the entanglement between  $R_1$  and  $R_2$  significantly reduces the query complexity to  $\mathcal{O}(2^{n/2})$ , translating to a total temporal complexity of  $\mathcal{O}(2^{n/2+1})$ . Beginning with qubit initialization, the algorithm first uses Hadamard gates to equally distribute probability among all DV addresses on  $R_1$ . It is followed by phase gating, diffusion gating, and data for DV validation to store corresponding entangled computation states on  $R_2$ . Grover search then follows by performing the “inversion about average”

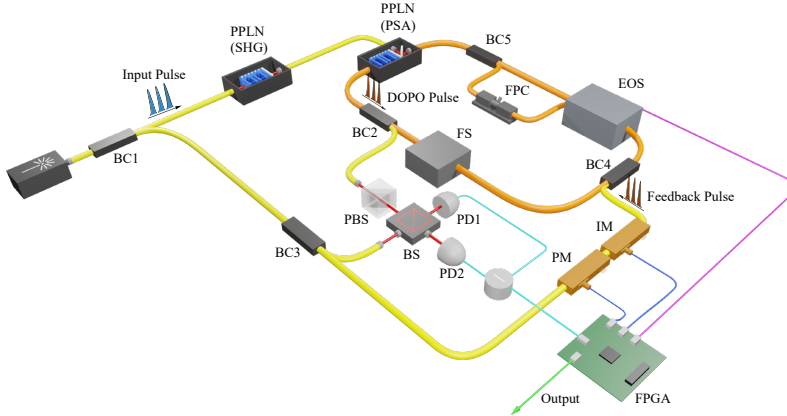


**Figure 1.** Experimental schematic of an optical implementation of SHA-1 DV search algorithm. FPGA: field-programmable gate array; PM: phase modulator; IM: intensity modulator; EOS: electro-optical switch; FPC: fiber polarization controller; FS: fiber stretcher; PD: photon diode; BS: beam splitter; PBS: polarizing beam splitter.

to elicit the address states with the greatest magnitude of probability, which associate with valid DV states leading to collisions in  $R_2$ . An algorithmic simulation based on pure-state quantum evolution simulation package [19] verifies the validity of the algorithm on  $2^7$  space.

The proposed algorithm is optically implementable on degenerate optical parametric oscillators (DOPOs). These parametric oscillators are coherent laser pulses running in a ring optical cavity. The carrier phase and the polarization direction of each such pulse are inseparable in a sense equivalent to the inseparability of two quantum entangled states [20]. The coherence of these pulsed DOPOs can be maintained by phase-sensitive amplification (PSA) in nonlinear optical crystals. The scale of pulse width being as short as picosecond, a sufficiently long ring cavity can store arbitrarily qubit-long information on a train of DOPOs, where the entangled  $R_1$  and  $R_2$  data are encoded on the phases and directions of the DOPOs, respectively. By virtue of their coherent scalability, these special pulses have been employed to realize graph-theoretic algorithms on the so-called coherent Ising machine [21, 22, 23] as well as Shor’s factoring algorithm [24]. We show here that all the quantum gating and feedback machinery involved in DV searching described above are entirely implementable via optical means and auxiliary classical computation. In other words, the proposed algorithm is immediately accessible, where a viable experimental setup is illustrated in Fig. 1. Before we describe the setup in details in Sec. 5, we explain the SHA-1 hashing and its valid attacks in Sec. 2, which is followed by the descriptions of the quantum algorithm and its simulated verification in Sec. 3. The conclusions are given in Sec. 6.

## 2. Classical collision attacks of SHA-1

The cryptographic hash function takes an input of a 512-bit block and converts it into a 160-bit hash value output. Messages of lengths less than  $2^{64}$  bits long are first chopped

into 512-bit blocks. Following the Merkle-Damgard construction [25], each block is then sequentially fed into a compression loop, combining with a 160-bit input chaining variable vector into a new 160-bit output vector during, where the new vector will be used as the input for compressing the next block in the next iteration. The chaining variables are set initially to fixed values while the final chaining values generated from compressing the last block forms the hash value, constituting the encryption process of SHA-1. In the following, we simplify the study by considering only one-block long messages.

Good cryptographic hash functions should be “highly sensitive” to the messages, meaning that a small variation in the message content results in a highly different hash output. Collision attacks occur when two different messages generate the same hash value. In other words, searching for collision attacks is to find a message that shares the same hash value, while being distinct from the intended message. Therefore, collision attack search serves to validate the security of a hashing process. For SHA-1, its security was bleached in 2005 [4] when it was successfully attacked through a collision realized by a well-constructed differential path. In contrast to thorough brute-force search in the space of all possible message inputs, the differential path construction is, generally speaking, a bit-shifting process of the differences between the values adopted by consecutive chaining variables. Uncovering the differential path essentially reworks the chaining-variable dependent compression loop such that a message with the same hash value can be found without repetitively executing the compression process to verify the hash output.

Therefore, the clever method has greatly reduced the time complexities of finding collision attacks but constructing the differential path is still computation intensive. To further mitigate the complexity, one introduces disturbance vectors (DVs) defined as those difference vectors that are reduced to zero after six compression iterations between the colliding message and the original. In other words, such DVs indicate the starting points of six-step local collisions, which are characteristic of the SHA-1 hashing algorithm. One typical construction of such local collisions was shown in Ref. [3], where the chaining variables are reversely computed from the DVs that lead to local collisions.

More specifically, a DV is a vector  $v = (v_0, v_1, v_2, \dots, v_{79})$  comprising eighty 32-bit long words, i.e. each  $v_i = (x_0^i x_1^i x_2^i \dots x_{31}^i)$  is a vector of binary numbers  $x_k^i \in \{0, 1\}$ . These eighty words are not entirely arbitrary but are correlated to each other through the rule of message expansion amongst the 16-word partitions,

$$v_i = (v_{i-3} \oplus v_{i-8} \oplus v_{i-14} \oplus v_{i-16}) \ll 1, \tag{1}$$

where  $\oplus$  denotes bitwise addition. In other words, the expansion rule confines the space complexity for each  $v$  to  $\mathcal{O}(2^{16 \times 32})$ . For efficient collision search, only DVs with low Hamming weight  $w$  in each component  $v_i$  of  $v$ , i.e. those  $v_i$  with a small number of  $x_k^i$  being one, are considered to constrain the size of search space. Ref. [4] use heuristics to further confine their search space to reduce the search complexity: only DVs with Hamming weight concentrated on the beginning and end of each component, e.g.  $x_0^i, x_1^i, x_{30}^i$ , and  $x_{31}^i$  being one and the rest zero, are tested. The search space is overall reduced to  $\mathcal{O}(2^n)$  where  $n = 16\lambda$ , and  $\lambda$  is the bit weight describes the range of  $k$  that  $x_k^i$  could be 1. A recent analysis of cost functions has further improved the space complexity to  $65 \times \binom{512}{w}$  where  $w$  is the Hamming weight [9].

It can be noticed from Eq. (1) that the bits of a DV are not independent; rather, the second and subsequent words of each DV are dependent on the first word.

Therefore, if the valid DVs are juxtaposed as columns where each row denotes a word of certain Hamming weight, they will be tabulated in a matrix where the appearances of their first words will depart from each other by a few rows [9]. According to such a scheme of tabulation, valid DVs can be classified into two types. Searching for the locations of these first word appearances would be the goal of a practical setup discussed in Sec. 4.

### 3. Quantum algorithm for seeding disturbance vector

With the advent of quantum computer, the so-called quantum supremacy over classical algorithms is achieved when the unique features of quantum systems, such as superpositions and entangled states, are taken advantage of to obtain computing parallelism not available to classical computing machinery. From the perspective of complexity, this parallelism is rendered as a reduction across different complexity classes, often from the exponential class to the polynomial class. We see from the last section that classical collision search, though having already its complexity reduced through the assistance of heuristics, remains a hard problem due to the vast search space. In the following, we present our quantum search algorithm for a DV seed out of which would grow a collision in SHA-1 hash value.

As we discussed in the last section, characterizing a DV requires the knowledge of any sixteen consecutive components  $(v_i, \dots, v_{i+15})$  by employing the forward (or backward) message expansion formula. In particular, we can characterize all possible DVs by exhausting on the first sixteen components  $(v_0, \dots, v_{15})$ . Following the classical studies of SHA-1 collision searching, we assume a low bit weight  $\lambda$  for the occurrences of valid DVs such that the candidate DVs can be expressed as the concatenation  $\mu = X^0 X^1 \dots X^{15}$  of 16  $\lambda$ -bit long strings  $X^i = x_0^i x_1^i \dots x_{\lambda-1}^i$ . We adopt the convention that the leftest bit  $x_0^0$  to be the least significant bit. For a hardware perspective, the candidate DVs are stored in a  $n$ -qubit quantum work register  $R_W$ , whose address is specified by another  $n$ -qubit quantum control register  $R_C$  it entangles with. An eigenvector  $|\psi_C, \psi_W\rangle$  then denotes an associated pair of address data and content data for each candidate DV. The concurrency of the quantum algorithm is thus reflected by the possibility of searching for collision-inducing DVs in a linear superposition of these eigenvectors.

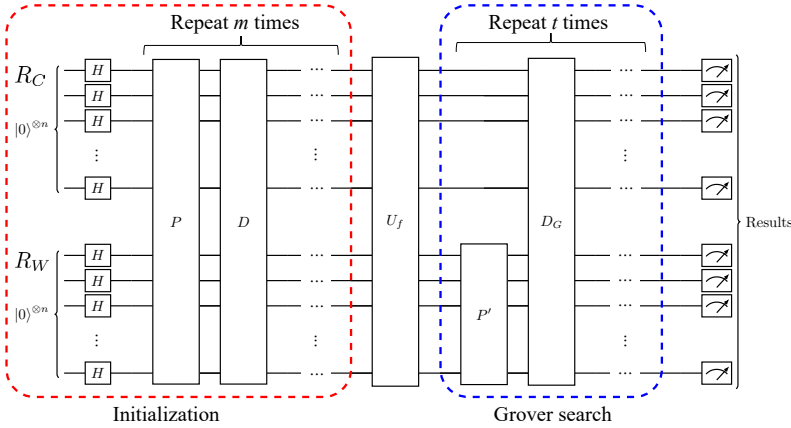


**Figure 2.** An implementation of the DV-search algorithm by a quantum circuit. Starting with  $n$  qubits with each state  $|0\rangle$  in the first and work registers. The number of repeat times of Grover search  $t = \mathcal{O}(2^{n/2})$ . Initialization and Grover search will operate on these direct product states which turn the qubits system representing an entangled state containing marked states with larger norms of their coefficients. Then, measuring all the qubits and readouts will give the information of valid DVs.

In other words, for the SHA-1 hashing, both  $R_C$  and  $R_W$  registers are  $n = 16\lambda$  qubit long, rendering the DV search space  $S = \{\zeta | 0 \leq \zeta \leq 2^n - 1\}$ . Encoding the classical data of  $S$  into the Hilbert space, each of the two registers states are distributed with equal probability using the Hadamard gates before we could proceed to the next operation, as shown in Fig 2. To generate the entanglement between  $R_C$  and  $R_W$  such that the DV data registered in  $R_W$  is directly correlated with the address in  $R_C$ , a set of phase gates  $P$  and diffusion gates  $D$  (shown as the red dashed box of Fig. 2) is applied. That is, the joint eigenstates of the quantum computer would have the address value record the original value of candidate DVs so that subsequent operations on  $R_W$  would leave the register  $R_C$  unchanged and the  $R_C$  states that remain would contain the value of valid DVs associated with hashing collisions.

Conventionally, the correlation between  $R_C$  and  $R_W$  is formed through entanglement operations implemented using elementary logical gates such as  $\sqrt{i}$ SWAP gates based on the superexchange (SE) interaction, which were used for generating Einstein-Podolsky-Rosen (EPR) pairs among ultracold Rb atoms [26] and Greenberger-Horne-Zeilinger (GHZ) state [27]. The SE interaction permits long-range correlation between two configurations of two spin particles inside a double-well potential. However, such ubiquitous methods are not suitable for the scenario here because of the extremely sophisticated combinations of quantum logical gates. The phase and diffusion gates in our approach realize approximately the same entangled state except for a tail part  $|\psi\rangle$  of negligible probability without heavily taxing the complexity of the entire algorithm. Once the correlation is generated, a DV-validity authenticating gate  $U_f$  is applied to change the data in the work register  $R_W$  to the hashed value:  $|\Psi_f\rangle = U_f |\Psi_0\rangle$  corresponding to the entangled data in the control register  $R_C$ . Finally, a Grover search is executed to select the states with the colliding hashed value. In the subsections below, we detail the quantum operations needed to implement the multiple step introduced above.

### 3.1. State preparations on the registers

Before the machine can correctly select the valid DVs from the control register, it is prepared with an initialization process that converts the preliminary zero state  $|0\rangle$  of the  $2n$  qubits into a superposition of equally weighted candidate states, using Hadamard gates:

$$|\Psi_0\rangle = \frac{1}{\sqrt{N}} \sum_{\alpha=0}^{\sqrt{N}-1} \sum_{\beta=0}^{\sqrt{N}-1} |\alpha, \beta\rangle, \quad (2)$$

where  $N = 2^{2n}$  is the total number of possible combinations of  $R_C$  and  $R_W$  data. Since candidate DVs serve both as the address in  $R_C$  and the work content in  $R_W$ , only the eigenstates with identical  $R_C$  and  $R_W$  data are wanted. The phase gates  $P$  and the diffusion gates  $D$ , indicated by the red dashed square in Fig 2, are therefore used to filter out the undesired eigenstates to retain the selection

$$|\Psi\rangle = \frac{1}{N^{1/4}} \sum_{\zeta=0}^{\sqrt{N}-1} |\zeta, \zeta\rangle, \quad (3)$$

The undesired states constitute a tail state  $|\psi\rangle$ , which would contribute a negligible probability after multiple iterations of  $DP$  gating, i.e. after  $m$  iterations on the initial state, we have

$$(DP)^m |\Psi_0\rangle = c|\Psi\rangle + c'|\psi\rangle, \quad (4)$$

where  $c, c' \in \mathbb{R}$  and  $|c|^2 \gg |c'|^2$ . To show this, we can refer to the proof steps of the effectiveness of the Grover search [12] by treating the phase and diffusion gating here as inversion about average and diffusion of probabilities among all eigenstates, respectively. In other words, the operation is a generalized Grover search that amplifies the probabilities of multiple eigenstates instead of a single one, at the end of which the remaining states are the ones that have formed entanglement between  $|\zeta\rangle$  in  $R_C$  and  $|\zeta\rangle$  in  $R_W$ , i.e.

$$(DP)^m |\Psi_0\rangle \approx |\Psi\rangle. \quad (5)$$

The phase and diffusion gating is readily decomposable into elementary single- and double-qubit gates [28, 29]. Their full  $N \times N$  matrix representations are

$$[P]_{ij} = \begin{cases} 0 & i \neq j \\ -1 & i = j = \sqrt{N}\zeta + \zeta + 1 \\ 1 & \text{otherwise} \end{cases} \quad [D]_{ij} = \begin{cases} \frac{2}{N} & i \neq j \\ \frac{2}{N} - 1 & i = j \end{cases}, \quad (6)$$

where  $\zeta$  ranges over 0 to  $\sqrt{N} - 1$ . The decomposition of the phase gate can be accomplished in two step: (i) decompose  $P$  into the product  $P = \prod_{\nu=0}^{\sqrt{N}-1} \Lambda_\nu$  where the elements of the  $\Lambda_\nu$  matrices are

$$[\Lambda_\nu]_{ij} = \begin{cases} 0 & i \neq j \\ -1 & i = j = \sqrt{N}\nu + \nu + 1; \\ 1 & \text{otherwise} \end{cases} \quad (7)$$

(ii) decompose these  $\Lambda^\nu$  into elementary controlled gates such as CZ and  $Z$ -rotation gates [30]. To decompose the diffusion gate  $D$ , (i) first rewrite it in terms of the outer product of the initial machine state:  $D = 2|\Psi_0\rangle\langle\Psi_0| - I$ ; (ii) then using the tensor

product  $H^{\otimes 2n}$  of Hadamard gates  $H$ , one can express  $D = H^{\otimes 2n} (2|0\rangle\langle 0| - I) H^{\otimes 2n}$  where the middle factor is just a  $2n$ -qubit CZ gate. The latter is again further decomposable into double-qubit CZ gates and  $Z$ -rotation gates.

After the entanglement, a DV-validity authenticating gate  $U_f$  is operated on the machine state to switch the eigenstates of the work register  $R_W$  to its hashed value, i.e.

$$U_f|\zeta, \zeta\rangle = |\zeta, f(\zeta)\rangle, \quad (8)$$

where the SHA-1 authenticating function  $f : \mathbb{N} \times \mathbb{N} \rightarrow \mathbb{N}$  assigns a zero value if  $\zeta$  is a collision-inducing DV or otherwise a non-zero value  $\mu_\zeta$ . For example, if  $\xi$  is such a valid DV,  $U_f|\xi, \xi\rangle = |\xi, 0\rangle$ . When  $U_f$  operates on all eigenstates, the final machine state has the eigenstates partitioned into two groups:

$$|\Psi_f\rangle \approx \frac{1}{N^{1/4}} \left( \sum_{\zeta \in V} |\zeta, 0\rangle + \sum_{\zeta \notin V} |\zeta, \mu_\zeta\rangle \right), \quad (9)$$

where  $V$  indicates the set of all valid DVs.

### 3.2. Grover search

The second major part of the algorithm is a standard Grover search, indicated by the blue dashed square in Fig 2, which is also implementable using single- and double-qubit gates. The Grover search performed on the work register amplifies the probabilities of the states carrying specific data, which in our case is the zero value for valid DVs. In order to search for the zero states of  $R_W$ , it is necessary to redefine the inversion gate  $P_G$  as the tensor product  $I \otimes P'$ , where the phase gate  $P'$  is a  $\sqrt{N} \times \sqrt{N}$  matrix with elements

$$[P']_{ij} = \begin{cases} 0 & i \neq j \\ -1 & i = j = 1 \\ 1 & \text{otherwise} \end{cases}, \quad (10)$$

on the work register  $R_W$ . The diffusion gate

$$D_G = 2|\Psi_f\rangle\langle\Psi_f| - I, \quad (11)$$

though similar to the one in last section, is defined with  $|\Psi_f\rangle$  instead of  $|\Psi_0\rangle$ . After  $N^{1/4}$  iterations of  $D_G P_G$ , the probabilities of the states with valid DVs are amplified.

We have run a simulation of the collision-inducing DV searching algorithm with  $2n = 14$  qubits using a quantum evolution simulation package [19]. The machine states are initialized at  $|0\rangle$  and  $m = \lfloor 2^{n/2} \rfloor$  iterations of  $DP$  gating are applied. Figure 3 shows the probabilities of the three typical eigenstates  $|\xi, 0\rangle$ ,  $|\zeta, \zeta\rangle$ , and  $|\zeta', 0\rangle$  from Eq. (9) at every iteration of  $D_G P_G$  gating during the Grover search. The eigenstate  $|\xi, 0\rangle$  represents the case of valid DV  $\xi$  that would induce a hash collision, i.e.  $f(\xi) = 0$ ; the eigenstate  $|\zeta, \mu_\zeta\rangle$  where  $\zeta$  is not one of those valid  $\xi$  represents the case of non-valid DV; the eigenstate  $|\zeta', 0\rangle$  represents the tail state case where  $f(\zeta') = 0$  even though  $\zeta'$  is not a valid DV. Since the authenticating  $U_f$  is conducted outside of the quantum circuit, we have used  $|0, 0\rangle$  for the  $|\xi, 0\rangle$  case and  $|\zeta, \zeta\rangle$  for the  $|\zeta, \mu_\zeta\rangle$  case without loss of generality in the quantum simulation.

One can observe that before the Grover search begins, the tail state  $|\psi\rangle$  which comprises the  $|\zeta', 0\rangle$  eigenstates has the much suppressed probability  $1.024 \times 10^{-5}$  compared to the probability  $6.512 \times 10^{-3}$  of the valid-DV states and the regular



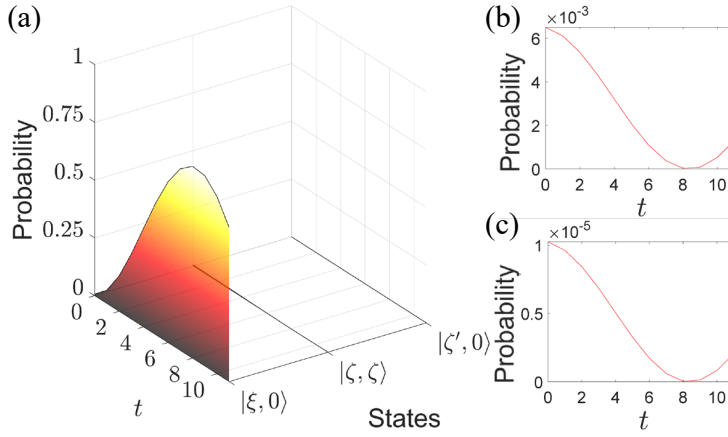


**Figure 3.** Probability variations of typical eigenstates of a simulation of the collision-inducing DV searching algorithm with  $2n = 14$  qubits, along with the number  $t \in \{1, 2, \dots, \lfloor 2^{n/2} \rfloor\}$  of Grover search iterations (applications of  $D_G P_G$  gates) where both the control register  $R_C$  and the work register  $R_W$  have  $n = 7$  qubits, using a quantum evolution simulation package [19]. In (a),  $|\xi, 0\rangle$  indicates the states with collision-inducing DV  $\xi$  which only equals zero in this simulation;  $|\zeta, \zeta\rangle$  the other states with non-zero  $\zeta$ ;  $|\zeta', 0\rangle$  the tail states with diminishing probability, although having  $R_W$  equals zero. The results show that the algorithm sufficiently amplifies the probability of the marked states  $|\xi, 0\rangle$ . (b) and (c) shows the magnified views of the probabilities of  $|\zeta, \zeta\rangle$  and  $|\zeta', 0\rangle$ , respectively.

non-valid-DV states. After Grover search begins, each iteration of  $D_G P_G$  gating further suppress the probability of  $|\psi\rangle$  to a negligible value; the magnified view of this probability is given in Fig. 3(c). Meanwhile, the state  $|\xi, 0\rangle$  has its probability be amplified to a significant value while the state  $|\zeta, \mu_\zeta\rangle$  experiences a great probability reduction (magnified view shown in Fig. 3(b)) during the  $D_G P_G$  gatings, although both of them start off from the same probability value. Therefore, the distinguishing ability of the valid disturbance vector from the non-valid in the proposed algorithm is verified.

### 3.3. Complexity estimation

According to classical computation theory,  $\mathcal{O}(2^\kappa)$  classical queries are required to compute all possible results encoded by  $\kappa$  classical bits in the worst case scenario. In contrast, the complexity metric that measures the DV-seeding quantum algorithm is contributed by the phase gating, the diffusion gating, and the Grover search that are characterized by a black box function, known as the query model[31, 32, 33]. The initialization using Hadamard gates and the following DV-authenticating operator  $U_f$ , whose complexity can be regarded as  $\mathcal{O}(1)$ , are excluded from the query searching part [15]. The phase gate  $P$  and diffusion gate  $D$  are admitted to have a query time  $m \approx 2^{n/2}$  which contributes a complexity  $\mathcal{O}(2^{n/2})$  of the operations  $DP$ . The Grover search is applied on the work register  $R_W$ , which contributes a query complexity of  $\mathcal{O}(2^{n/2})$  under the query time  $t = 2^{n/2}$ . Under the implementation of a quantum circuit, the number of quantum gates that implement the black-box operators is

polynomial, rather than exponential, in the number of input qubits. Since the *DP* step and the Grover search are sequential, the total query complexity of the algorithm is  $\mathcal{O}(2^{n/2+1})$  in the search space  $S = \{\zeta | 0 \leq \zeta \leq 2^n - 1\}$ , which is vastly sped up from the  $\mathcal{O}(2^n)$  queries for classical complexity.

#### 4. Specification on type-I DV

Current cryptographic studies have categorized the occurrences of valid DVs into two types, according to their clustering in certain subsets of the entire search space. Then given these category information, the quantum search of valid DVs can be confined to the subsets, which greatly reduces the search complexity. Specifically, the address of the first word of the type-I DVs, for instance, only appears in a  $2^5$  space out of  $2^{512}$  [9]. Our quantum algorithm described in last section can still apply to this scenario of restricted search space. Moreover, under the consideration of the limited quantum resources, the confinement of the search space significantly reduces the quantum resources, such as the number of qubits and elementary quantum gates employed in the quantum algorithm, by increasing the classical restriction.

All type-I DVs are contained in a table constructed from a set of consecutive 16-bit words  $\{v_i\}$ , which satisfies the message expansion relation Eq. 1, for each  $v_i$  represents a line. DVs in this type can be mapped into this table, operated by their unique bit-shift, starting from different lines. The table can be infinitely expanded forward or backward but is manually limited as it is sufficient to cover all type-I DVs found by previous works. Notice that it is possible to expand the rest part of a type-I DV after knowing its starting line, which can be used to further reduce the search space. In this case, the search space is shrunk from  $S$  into a deterministic table shown in Tab. 1, and the number of qubits in the control and work register are both  $n = 5$ . The initial state is shown in this form

$$|\Psi_0\rangle = \frac{1}{2^5} \sum_{\alpha=0}^{2^5-1} \sum_{\beta=0}^{2^5-1} |\alpha, \beta\rangle = \frac{1}{2^5} (|\Psi_T\rangle + |\psi\rangle), \quad (12)$$

where  $|\Psi_T\rangle$  is the summation of eigenstates  $|l, u_l\rangle$  listed in Tab. 1 and tail state  $|\psi\rangle$ . After applying the phase gates, diffusion gates, and DV-validity authenticating gate, the machine state  $|\Psi_f\rangle$  intends to contain these marked eigenstates  $|l, 0\rangle$  for  $l \in \{0, 1, 2, 3, 7, 11, 13, 17\}$ , with the probability of the tail state being diminished to zero. Then, the Grover search is acted on the system and amplifies the magnitudes of the marked eigenstates, which are the states expected to be measured.

**Table 1.** The eigenstates  $|l, u_l\rangle$  inside  $|\Psi_T\rangle$  based on the table of the expanded type-I DV.

The first 18 lines of the Type-I Disturbance vector	Order	$ l\rangle \in R_C$	Starting points of 6-step local collisions	$ u_l\rangle \in R_W$	$ l, u_l\rangle$
-----	1	$ 0\rangle$	0	$ 0\rangle$	$ 0, 0\rangle$
-o-----	2	$ 1\rangle$	6	$ 6\rangle$	$ 1, 6\rangle$
-----	3	$ 2\rangle$	0	$ 0\rangle$	$ 2, 0\rangle$
-o-o-----	4	$ 3\rangle$	10	$ 10\rangle$	$ 3, 10\rangle$
o-----	5	$ 4\rangle$	1	$ 1\rangle$	$ 4, 1\rangle$
o-----	6	$ 5\rangle$	1	$ 1\rangle$	$ 5, 1\rangle$
o-o-----	7	$ 6\rangle$	5	$ 5\rangle$	$ 6, 5\rangle$
-o-----	8	$ 7\rangle$	2	$ 2\rangle$	$ 7, 2\rangle$
-----	9	$ 8\rangle$	0	$ 0\rangle$	$ 8, 0\rangle$
-o-----	10	$ 9\rangle$	6	$ 6\rangle$	$ 9, 6\rangle$
o-----	11	$ 10\rangle$	1	$ 1\rangle$	$ 10, 1\rangle$
o-----	12	$ 11\rangle$	1	$ 1\rangle$	$ 11, 1\rangle$
o-----	13	$ 12\rangle$	1	$ 1\rangle$	$ 12, 1\rangle$
-----	14	$ 13\rangle$	0	$ 0\rangle$	$ 13, 0\rangle$
-----	15	$ 14\rangle$	0	$ 0\rangle$	$ 14, 0\rangle$
-o-----	16	$ 15\rangle$	2	$ 2\rangle$	$ 15, 2\rangle$
-----	17	$ 16\rangle$	0	$ 0\rangle$	$ 16, 0\rangle$
o-o-----	18	$ 17\rangle$	5	$ 5\rangle$	$ 17, 5\rangle$

### 5. Implementation using DOPO network

We demonstrate an optical-based implementation of the quantum algorithm by employing a network of degenerate optical parametric oscillators (DOPOs), as illustrated in Fig. 1. Each DOPO pulse has two degrees of freedom: in-phase (0 or  $\pi$ ) and polarization (horizontal or vertical), shown in Fig. 4(b) and (c), representing a two-qubit eigenstate. Following this construction, the control  $R_C$  and work register  $R_W$  are represented by the in-phase and polarization of the DOPO pulses train running in the orange ring optical fiber cavity in Fig. 1. The implementation of the entangled desired state in Eq. 3 requires  $2^n$  groups of  $n = 16\lambda$  DOPO pulses and each group of pulses represents a coupled eigenstate  $|\zeta, \zeta\rangle$ . Totally  $n \cdot 2^n$  number of DOPO pulses are required in the cyclic fiber, and the states in the cavity are shown in Fig. 4(a). The time-multiplexed DOPO network is formed by the pump-powered PSA in the single fiber-ring containing pulses with the round trip time  $T_{rt}$ .

A 1536 nm pulsed laser source is used to generate pulses and power the DOPO in the ring cavity. The beam combiner (BC) 1 splits the source into two paths, one of which behaves as input pulses of the machine and passes through a second-harmonic generation (SHG) process by a PPLN. The other is split again by BC3 to serve as a local oscillator (LO) for balanced homodyne detection (BHD) and feedback pulses after being modulated by phase and intensity modulators controlled by FPGA [24], shown as the blue control lines in Fig. 4. The input signal after SHG is used to synchronously pump the PPLN for a PSA in the fiber ring. All the DOPO pulses

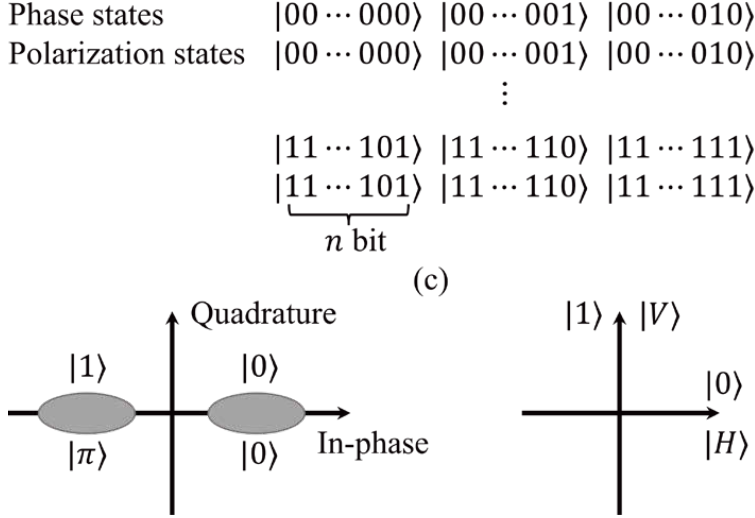


**Figure 4.** (a)The initialized states of  $n \cdot 2^n$  DOPO pulses. Each double line represents one group of DOPO pulses, and all information on the starting point of the first word of DVs are encoded by groups of phase and polarization states, respectively; (b)(c)the representation relations between the polarization and phase of DOPO and represented qubit state.

are generated with horizontal polarization initially, due to the type 0 phase matching proposition of the PSA process [34]. The optical switch, which is realized by an EOS and a FPC, is connected for allowing horizontally polarized pulses to pass through initially. The EOS is initially switched to disconnected with the FPC and controlled by the FPGA through the magenta control line in Fig. 4. A fiber stretcher is connected for stabilizing the state of pulses and maintaining the length of the circulated cavity. In other words, the cavity length compensates for the relative phase difference, fixed at 0 or  $\pi$ , between the signal pulse and pump pulse, which are maintained synchronously [24].

The initialization of the machine is achieved by horizontally polarized and in-phase 0 DOPO pulses representing the initial  $|0\rangle$  state. To implement the iterations of *DP* gating and achieve the entanglement, the FPGA controls the IM and PM to adjust the feedback pulses to tune the cavity state into the machine state in Eq. 5. The tail state  $|\psi\rangle$  is neglected because we selectively tune the phase and polarization of each pulse in a group to represent the entangled desired state directly. The polarization of each pulse is recorded in the FPGA and will not be physically changed before performing a measurement of the machine. Then, a BHD measures the in-phase component  $c_j$  of each pulse, which collects the phase information  $\zeta$  of each group of pulses and sends to the FPGA [?, 24]. The phase part of the DOPO pulse is 0 or  $\pi$  corresponding to  $c_j$  is positive or negative, respectively. The FPGA uses the inputs of combined phase and polarization information  $(\zeta, \zeta)$  to control the IM and PM to modulate the corresponding feedback pulses  $f_i$  that interfere with the original pulses and tune the in-phase components of each group of pulses [35, 36]. The state represented by the group of pulses is changed from the eigenstate  $|\zeta, \zeta\rangle$  to the hashed

state  $|\zeta, f(\zeta)\rangle$ , which implements the DV-validity authenticating gate  $U_f$ .

The Grover search is realized by a polarization filter that retains the entire group of pulses with pure horizontal polarization. Before performing a measurement, the FPGA controls the EOS to adjust the polarization of groups of DOPO into their corresponding states  $|f(\zeta)\rangle$ . The machine state shown in Eq. 9 is finally presented by the DOPO trains in the optical cavity and sent to the BHD. As the polarizations of DOPOs are changed before they are measured, the Grover search then is equivalent to a PBS, where all the states with any vertical polarization will be broken and with pure horizontal polarization will be preserved and sent into BHD, which is equivalent to the Grover search to get the states with  $|0\rangle$  in the work register  $R_W$ .

## 6. Conclusions

We propose a quantum algorithm for seeding disturbance vectors, which describe differential paths that would successfully lead to collisions on SHA-1 hashing results. The algorithm has a query complexity of  $\mathcal{O}(2^{n/2+1})$  where  $n$  is the number of qubits that encodes the addresses of disturbance vectors. A simulation of the algorithm is presented, successfully verifying the algorithmic validity where the collision-inducing vectors have their probabilities amplified under the algorithmic steps of phase-diffusion gating and Grover search. We further reduce the search space by confining the candidate disturbance vectors into a specific type, within which the quantum algorithm is still valid. In addition, an optical implementation of our algorithm is proposed using a DOPO network of coherent laser pulses running in a ring fiber cavity. These results highlight that the proposed algorithm is imminently implementable and is able to find the same disturbance vectors with lower computational complexity than its classical counterparts.

## Reference

- [1] Preneel B 2010 The first 30 years of cryptographic hash functions and the nist sha-3 competition *Cryptographers' track at the RSA conference* (Springer) pp 1–14
- [2] Standard S H 1995 *National Institute of Standards and Technology* **17** 15
- [3] Wang X, Yu H and Yin Y L 2005 Efficient collision search attacks on sha-0 *Annual International Cryptology Conference* (Springer) pp 1–16
- [4] Wang X, Yin Y L and Yu H 2005 Finding collisions in the full sha-1 *Annual international cryptology conference* (Springer) pp 17–36
- [5] Biham E, Chen R, Joux A, Carribault P, Lemuet C and Jalby W 2005 Collisions of sha-0 and reduced sha-1 *Annual International Conference on the Theory and Applications of Cryptographic Techniques* (Springer) pp 36–57
- [6] Stevens M 2013 New collision attacks on sha-1 based on optimal joint local-collision analysis *Annual International Conference on the Theory and Applications of Cryptographic Techniques* (Springer) pp 245–261
- [7] Szydlo M and Yin Y L 2006 Collision-resistant usage of md5 and sha-1 via message preprocessing *Cryptographers' Track at the RSA Conference* (Springer) pp 99–114
- [8] Stevens M and Shumow D 2017 Speeding up detection of {SHA-1} collision attacks using unavoidable attack conditions *26th USENIX Security Symposium (USENIX Security 17)* pp 881–897
- [9] Manuel S 2011 *Designs, Codes and Cryptography* **59** 247–263
- [10] Arute F, Arya K, Babbush R, Bacon D, Bardin J C, Barends R, Biswas R, Boixo S, Brandao F G, Buell D A *et al.* 2019 *Nature* **574** 505–510
- [11] Shor P W 1994 Algorithms for quantum computation: discrete logarithms and factoring *Proceedings 35th annual symposium on foundations of computer science* (Ieee) pp 124–134
- [12] Grover L K 1996 A fast quantum mechanical algorithm for database search *Proceedings of the twenty-eighth annual ACM symposium on Theory of computing* pp 212–219

- [13] Grassl M, Langenberg B, Roetteler M and Steinwandt R 2016 Applying grover’s algorithm to aes: quantum resource estimates *Post-Quantum Cryptography* (Springer) pp 29–43
- [14] Lavor C, Manssur L and Portugal R 2003 *arXiv preprint quant-ph/0301079*
- [15] Durr C and Hoyer P 1996 *arXiv preprint quant-ph/9607014*
- [16] Dobraunig C, Eichlseder M and Mendel F 2015 Analysis of sha-512/224 and sha-512/256 *International Conference on the Theory and Application of Cryptology and Information Security* (Springer) pp 612–630
- [17] Mendel F, Nad T and Schl affer M 2013 Improving local collisions: new attacks on reduced sha-256 *Annual International Conference on the Theory and Applications of Cryptographic Techniques* (Springer) pp 262–278
- [18] Hosoyamada A and Sasaki Y 2021 Quantum collision attacks on reduced sha-256 and sha-512 *Annual International Cryptology Conference* (Springer) pp 616–646
- [19] Johansson J R, Niaton P D and Nori F 2012 *Computer Physics Communications* **183** 1760–1772
- [20] You Z, Wang Y, Tang Z and Ian H 2021 *JOSA B* **38** 1798–1805
- [21] Inagaki T, Haribara Y, Igarashi K, Sonobe T, Tamate S, Honjo T, Marandi A, McMahon P L, Umeki T, Enbutsu K *et al.* 2016 *Science* **354** 603–606
- [22] Marandi A, Wang Z, Takata K, Byer R L and Yamamoto Y 2014 *Nature Photonics* **8** 937–942
- [23] McMahon P L, Marandi A, Haribara Y, Hamerly R, Langrock C, Tamate S, Inagaki T, Takesue H, Utsunomiya S, Aihara K *et al.* 2016 *Science* **354** 614–617
- [24] Li M, Wang W, Tang Z and Ian H 2022 *arXiv preprint arXiv:2205.11926*
- [25] Merkle R C 1979 *Secrecy, authentication, and public key systems*. (Stanford university)
- [26] Trotzky S, Cheinet P, Folling S, Feld M, Schnorrberger U, Rey A M, Polkovnikov A, Demler E A, Lukin M D and Bloch I 2008 *Science* **319** 295–299
- [27] Song C, Xu K, Liu W, Yang C p, Zheng S B, Deng H, Xie Q, Huang K, Guo Q, Zhang L *et al.* 2017 *Physical review letters* **119** 180511
- [28] Barenco A, Bennett C H, Cleve R, DiVincenzo D P, Margolus N, Shor P, Sleator T, Smolin J A and Weinfurter H 1995 *Physical review A* **52** 3457
- [29] Shende V V, Bullock S S and Markov I L 2006 *IEEE Transactions on Computer-Aided Design of Integrated Circuits and Systems* **25** 1000–1010
- [30] Mandviwalla A, Ohshiro K and Ji B 2018 Implementing grover’s algorithm on the ibm quantum computers *2018 IEEE international conference on big data (big data)* (IEEE) pp 2531–2537
- [31] Ambainis A 2000 Quantum lower bounds by quantum arguments *Proceedings of the thirty-second annual ACM symposium on Theory of computing* pp 636–643
- [32] Ambainis A 2006 *Journal of Computer and System Sciences* **72** 220–238
- [33] Bernstein E and Vazirani U 1997 *SIAM Journal on computing* **26** 1411–1473
- [34] Andrekson P A and Karlsson M 2020 *Advances in Optics and Photonics* **12** 367–428
- [35] Okawachi Y, Yu M, Jang J K, Ji X, Zhao Y, Kim B Y, Lipson M and Gaeta A L 2020 *arXiv preprint arXiv:2003.11583*
- [36] Marandi A, Leindecker N C, Vodopyanov K L and Byer R L 2012 *Optics express* **20** 19322–19330